academicJournals

Vol. 10(2), pp. 41-52, 30 January, 2015
DOI: 10.5897/SRE2014.5831
Article Number: D9EAA2649787
ISSN 1992-2248

http://www.academicjournals.org/SRE

Scientific Research and Essays

Full Length Research Paper

Laminar free and forced convection cooling of a semi permeable open cavity

C. A. Chaves[1*], W. Q. Lamas[2], J. R. Camargo[1], F. J. Grandinetti[1], C. A. C. Altemani[3]

[1]Mechanical Engineering Department, University of Taubaté, Rua Daniel Danelli, s/nº - Jardim Morumbí 12060-440 - Taubaté - SP - Brazil.
[2]Mechanical Engineering Department and Department of Basic and Environmental Sciences (School of Engineering at Lorena), University of Taubaté and University of Sao Paulo, Brazil.
[3]Mechanical Engineering Department, University of Campinas - Campinas - SP - Brazil.

Received 5 February, 2014; Accepted 19 January, 2015

Heat transfer inside a semi porous two-dimensional rectangular open cavity was numerically investigated. The open cavity comprises two vertical walls closed to the bottom by an adiabatic horizontal wall. One vertical wall is a porous and an inflow of fluid occurs normal to it. The other wall transfers a uniform heat flux to the cavity. It shows how natural convection effects may enhance the forced convection inside the open cavity. The main motivation for the work is its application for electronic equipment where frequently the devices used for the electronic equipment cooling are based on natural and forced convection. Governing equations are expressed in Cartesian coordinates and numerically handled by a finite volume method. Results are presented for both local and average Nusselt numbers at the heated wall and for the isotherms and streamlines of the fluid flowing inside the open cavity as a function of Reynolds number ranging from 1 to 100, Grashof number ranging from 0 to 10^{+7} and the aspect ratio number of the open cavity equal 2, 4 and 8. The results obtained show that the forced convection inside the semi-porous open cavity studied may be greatly enhanced by natural convection effects.

Key words: Computational simulation, electronic equipment cooling, finite volume, natural convection, open cavity; porous media.

INTRODUCTION

The heat transfer in enclosures has been studied for a variety of engineering applications. Results have been presented in research surveys (Bruchberg et al., 1976; Kakaç et al., 1987) and it has become a main topic in convective heat transfer textbooks (Bejan, 1984). Usually the enclosures are closed and natural convection is the single heat transfer mechanism. There are however, several applications in passive solar heating, energy conservation in building and cooling of electronic equipment, where open cavities are employed (Chan and Tien, 1985; Hess and Henze, 1984; Penot, 1982).

Frequently the devices employed for the cooling of electronic equipment are based on forced convection (Sparrow et al., 1985). Studies on Computational Fluid Dynamics (CFD) applied to analysis of electronics cooling had been developed in several works. Specially theory

*Corresponding author email: carlos.chaves@unitau.br, Tel/Fax: +55 12 3621-8002.

on natural convection in enclosures (Ostrach, 1972) and electronics cooling enclosure used as part of a larger telecommunication radar system (Boukhanouf and Haddad, 2010). Also studies of flow characteristics are done numerically with CFD and compared to experimental approaches, that is, manifolds that are widely used in electronic cooling equipment (Gandhi et al., 2012), shielded heat sink also widely used in that (Shaalan et al., 2012), and analysis to eliminate fan used in electronic device cooling (Nickell, 1997).

Several studies on natural convection in open cavities had been done. Steady-state natural convection taking place in rectangular cavities filled with air was studied both experimental and numerically in Bairi et al. (2007). A steady buoyancy-driven flow of air in a partially open square 2D cavity with internal heat source, adiabatic bottom and top walls, and vertical walls maintained at different constant temperatures was investigated numerically in Fontana et al. (2011). The numerical results of heat transfer calculations in an open cavity considering natural convection and temperature-dependent fluid properties were presented by Juarez et al. (2011). The natural convection occurring from open cavities was analysed by Prakash et al. (2012) in three different cavity shapes namely cubical, spherical and hemispherical geometries having equal heat transfer area. The thermal behaviour of airborne electronic equipment submitted to natural convection in closed parallelogrammic air-filled cavities was examined by Bairi et al. (2012). Also mixed convection in open cavity had been reviewed through several works.

Wong and Saeid (2009) investigated the opposing mixed convection arises from jet impingement cooling of a heated bottom surface of an open cavity in a horizontal channel filled with porous medium through a numerical study.

Stiriba et al. (2010) had analyzed the effects of mixed convective flow over a three-dimensional cavity that lies at the bottom of a horizontal channel through a numerical study, in which was found that the flow becomes stable at moderate Grashof number and exhibit a three-dimensional structure, while for both high Reynolds and Grashof numbers the mixed convection effects came into play.

A finite element analysis was performed on the conjugated effect of joule heating and magneto-hydrodynamic on double-diffusive mixed convection in a horizontal channel with an open cavity (Rahman et al., 2011).

Laminar mixed convective flow over a three-dimensional open cavity with heating from below at constant temperature was numerically simulated using direct numerical simulation and the most hydrodynamic and thermal aspects of the flow were presented by Stiriba et al. (2013). Magneto-hydrodynamic mixed convection in a lid driven cavity along with a heated circular hollow cylinder positioned at the centre of the cavity was studied numerically by Farid et al. (2013). Altemani and Chaves (1988) presented a numerical study of heat transfer inside a semi porous two-dimensional rectangular open cavity for both local and average Nusselt numbers at the heated wall and for the isotherms and streamlines of the fluid flowing inside the open cavity. Chaves et al. (2005) presented a numerical program in finite volumes applied to the transient natural convection heat transfer by double diffusion from a heated cylinder buried in a saturated porous medium. Chaves et al. (2008) presented a work where it was done a numerical analysis of the heat transfer inside a semi porous two-dimensional rectangular open cavity, where forced and natural convection where considered and the bottom and the opposite wall was heated.

This paper presents a continuation of work of Chaves et al. (2008) using the program development in Chaves et al. (2005) where numerical analysis of heat transfer was done inside a semi porous two-dimensional rectangular open cavity. It is constituted by two vertical parallel plates closed at the bottom by an adiabatic surf ace and open at the top, as indicated in Figure 1.

One of the vertical plates is porous and there is a fluid flow forced normal to it in order to cool the other vertical plate. This second plate transfer a uniform heat flux to the cavity. In addition to the forced convection, the analysis considered the influence of natural convection effects. Isotherms and streamlines are presented for the fluid flow inside the open cavity. Local and average Nusselt numbers are obtained for the uniformly heated plate for several values of aspect ratio to the parameters governing the heat transfer: Re_p and Gr.

METHODOLOGY

The conservation equation of mass, momentum and energy, as well as their boundary conditions, will be expressed for the system indicated in Figure 1. Due to the low velocities usually associated with permeable walls, the natural convection will be considered in the analysis. It is assumed that the flow is laminar and occurs under steady state conditions. The natural convection will be treated via the Boussinesq approximation, that is, density variations are accounted for only when they contribute to buoyancy forces. In this problem, the buoyancy term is obtained from the y momentum equation terms representing the pressure and body forces:

$$-\frac{\partial \mathrm{p}}{\partial \mathrm{y}} - \rho \cdot \mathrm{g} \tag{1}$$

The density is related to temperature according to the Boussinesq approximation (Patankar, 1980; Kundu and Cohen, 2008):

$$\rho = \rho_{\mathrm{p}} - \rho_{\mathrm{p}} \cdot \beta \cdot (\mathrm{T} - \mathrm{T_p}) \tag{2}$$

In Equation (2) T_p indicates the temperature of the fluid inlet at the porous wall and ρ_p the corresponding density. The pressure is now expressed in terms of a modified pressure defined as:

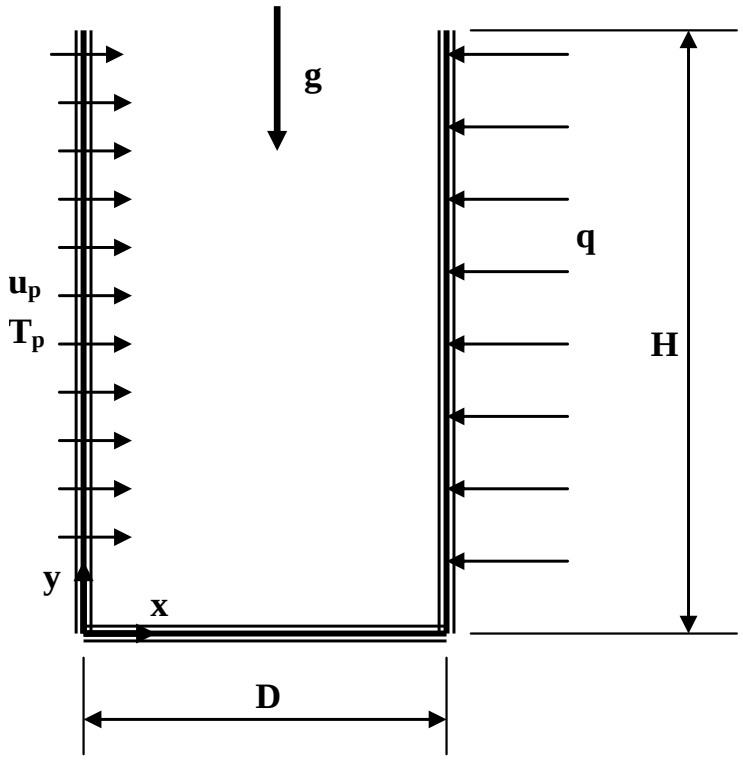

Figure 1. Coordinate system and thermal boundary conditions of the open cavity.

$$p^* = p + \rho_p \cdot g \cdot y \tag{3}$$

With Equations (2), (3), and (1) can be expressed by:

$$-\frac{\partial p^*}{\partial y} + \rho \cdot g \cdot \beta \cdot (T - T_p) \tag{4}$$

The second term in this equation relates the buoyancy forces to temperature differences ($T - T_p$). From this formulation, the density will be assumed constant and equals to ρ_p in all the equations, so that the subscript *p* may be deleted. It is also assumed that all the other properties of the fluid are constant. Viscous dissipation and compression work are not considered in the analysis, according to the low velocities, moderate temperature differences and laminar flow conditions assumed. In order to obtain the conservation equations in dimensionless form, the following variables were defined (Patankar, 1980; Kundu and Cohen, 2008):

$$X = \frac{x}{D} \ , \quad Y = \frac{y}{D} \tag{5a}$$

$$U = u \cdot \frac{D}{\nu} \ , \quad V = v \cdot \frac{D}{\nu} \tag{5b}$$

$$P = \frac{p^*}{\left(\frac{\rho \cdot \nu^2}{H^2}\right)} \ , \quad \theta = \frac{T - T_p}{\left(\frac{q \cdot D}{k}\right)} \tag{5c}$$

The equations expressing conservation of mass, x and y momentum and energy then become:

$$\frac{\partial U}{\partial X} + \frac{\partial V}{\partial Y} = 0 \tag{6}$$

$$U \cdot \frac{\partial U}{\partial X} + V \cdot \frac{\partial U}{\partial Y} = -\frac{\partial P}{\partial X} + \nabla^2 U \tag{7}$$

$$U \cdot \frac{\partial V}{\partial X} + V \cdot \frac{\partial V}{\partial Y} = -\frac{\partial P}{\partial Y} + \nabla^2 V + Gr \cdot \theta \tag{8}$$

$$U \cdot \frac{\partial \theta}{\partial X} + V \cdot \frac{\partial \theta}{\partial Y} = \frac{\nabla^2 \theta}{Pr} \tag{9}$$

In Equations (7) to (9) ∇^2 is the Laplace operator in Cartesian coordinates. These equations are coupled and present two independent parameters, Gr and Pr. The first is the modified

Grashof number, defined by Patankar (1980) and Sharma (2005):

$$Gr = \frac{g \cdot \beta \cdot q \cdot D^4}{k \cdot \nu^2} \quad (10a)$$

and the second is the Prandtl number of the fluid (Patankar, 1980; Sharma, 2005).

$$Pr = \frac{\mu \cdot C_p}{\kappa} = \frac{\nu}{\left(\frac{\kappa}{\rho \cdot C_p}\right)} \quad (10b)$$

At the three solid boundaries of the open cavity, the velocity components are null, except the velocity of injection of the fluid (U_p) at the porous wall. The thermal boundary conditions comprise a uniform (reference) temperature at the porous wall and a specified heat flux at the heated vertical wall. Expressed in dimensionless terms, the boundary conditions become:

$$X = 0 \; ; \; U_p = u_p \frac{D}{\nu} = Re_p \; ; \; V = 0 \; , \; \theta = 0 \quad (11a)$$

$$X = 1 \; ; \; U = 0 \; ; \; V = 0 \; , \; \frac{\partial \theta}{\partial X} = 1 \quad (11b)$$

$$Y = 0 \; ; \; U = 0 \; ; \; V = 0 \; , \; \frac{\partial \theta}{\partial Y} = 0 \quad (11c)$$

The dimensionless velocity component normal to the permeable wall $\left(u_p \cdot \frac{D}{\nu}\right)$ is one parameter of this problem and it will be denoted the porous wall Reynolds number, Re_p. The outflow boundary of the open cavity, at Y equal to H/D, is just a virtual boundary defining the calculation domain. In order to obtain a solution, two conditions must be satisfied at this boundary. First, there must be no backflow of fluid and second, there must be no diffusion from outside into the calculation domain. The first condition was verified checking the velocity profiles of each result obtained and discarding those results when a backflow was observed. The second was satisfied imposing artificially negligible partial derivatives of θ and U in the vertical direction at the outflow boundary. The velocity component V was corrected at the outflow boundary in order to satisfy the conservation of mass in the whole domain.

The problem presents four independent parameters: H/D, Pr, Re_p and Gr. For a fixed particular fluid, there are still three parameters governing the heat transfer: H/D, Re_p and Gr. In the present work, a single value, equal to 0.72, was assigned to the Prandtl number.

The differential Equations (6) to (9) together with their boundary conditions, Equation (11), comprise a coupled system involving the four variables U, V, P and θ. The equations were discretized using the control volume formulation described in Patankar (1980) and the solution was obtained employing the SIMPLE scheme. The convergence of the results was accepted when the relative change of the dependent variables was under 10^{-3}. From the velocity field solutions, a steam function defined as:

$$\psi = \int_0^Y U \cdot dY \quad (12)$$

was evaluated along lines X = constant, with ψ = 0 at X = Y = O.

From the solution of the temperature field, the local heat transfer coefficient at the heated wall and a corresponding Nusselt number were expressed as Patankar (1980) and Sharma (2005):

$$Nu(Y) = h(Y) \cdot \frac{D}{k} \quad , \quad h(Y) = \frac{q}{T_w(Y) - T_p} \quad (13)$$

Where T_W indicates the local temperature of heated wall. With the definition of the dimensionless temperature, Equation (5c), the Nusselt number becomes

$$Nu(Y) = \frac{1}{\theta_w(Y)} \quad (14)$$

An average Nusselt number for the heated wall was obtained from

$$\overline{Nu} = \overline{h} \cdot \frac{D}{k} \quad , \quad \overline{h} = \frac{q}{\overline{T}_w - T_p} \quad (15)$$

In Equation (15) $\overline{T}_w$ indicates the average heated wall temperature. Expressed in dimensionless variables, the average Nusselt number becomes.

$$\overline{Nu}(Y) = \frac{1}{\overline{\theta}_w} \quad (16)$$

Where $\overline{\theta}_w$ is evaluated by integrating the dimensionless temperature distribution along the heated wall:

$$\overline{\theta}_w = \frac{D}{H} \int_0^{H/D} \theta_w(Y) \cdot dY \quad (17)$$

The adequacy of the grid fineness employed in the results is presented in Figure 2, related to the average Nusselt number defined in Equation (16). In either the absence or the presence of natural convection effects, a grid of 30x30 was adequate for the aspect ratio of 2 used in most of our results. Increasing the number of grid points from 900 to 1,600 would change the average Nusselt number by 0.2% (Figure 2).

RESULTS AND DISCUSSION

Nusselt number distributions

Initially, just the effects of forced convection on the Nusselt number distributions will be considered to many aspect ratio H/D. The results presented in Figure 3 show that the Nusselt numbers increase with Re_p and that they attain a uniform value within the cavity. The increase of Nusselt number is due to both the larger fluid flow through the cavity and the effect of inertia forces, causing the streamlines to come relatively closer to the heated wall.

The comparison of the streamlines indicated in Figure 4 shows that a larger fraction of fluid flow occurs closer to

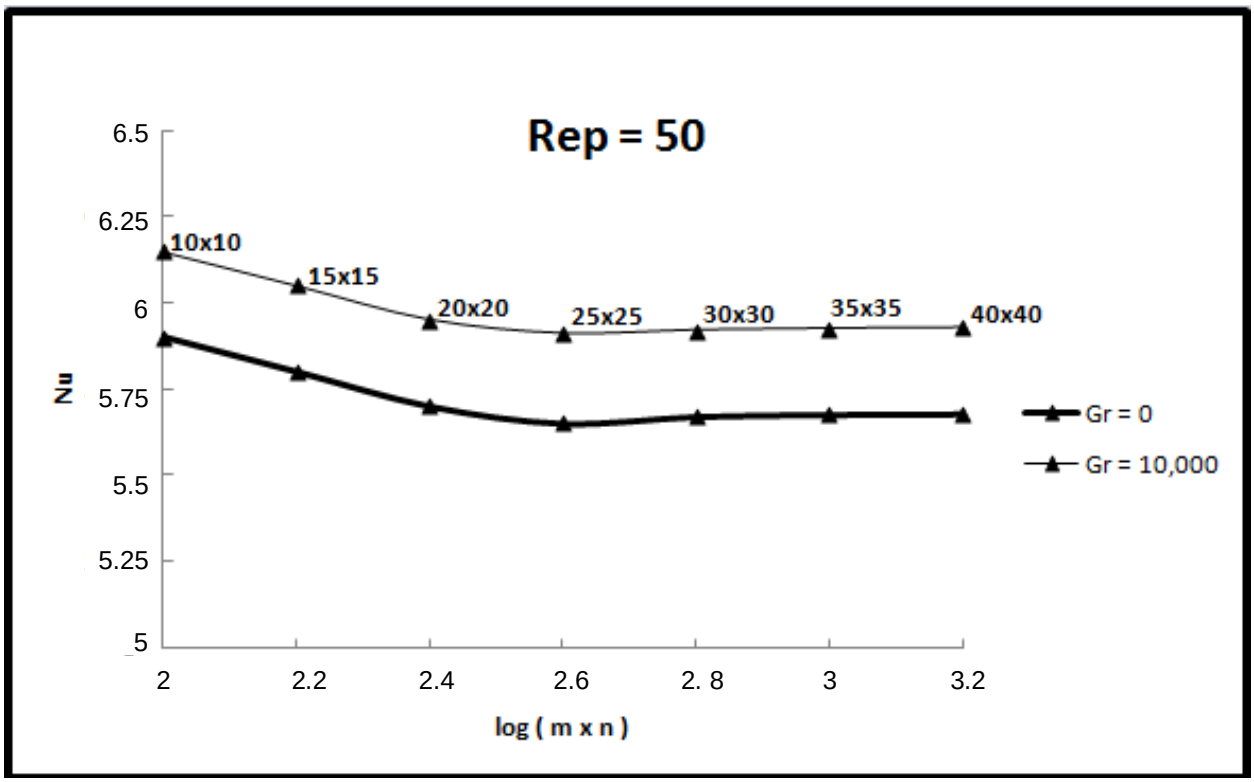

Figure 2. Adequacy of the grid fineness employed.

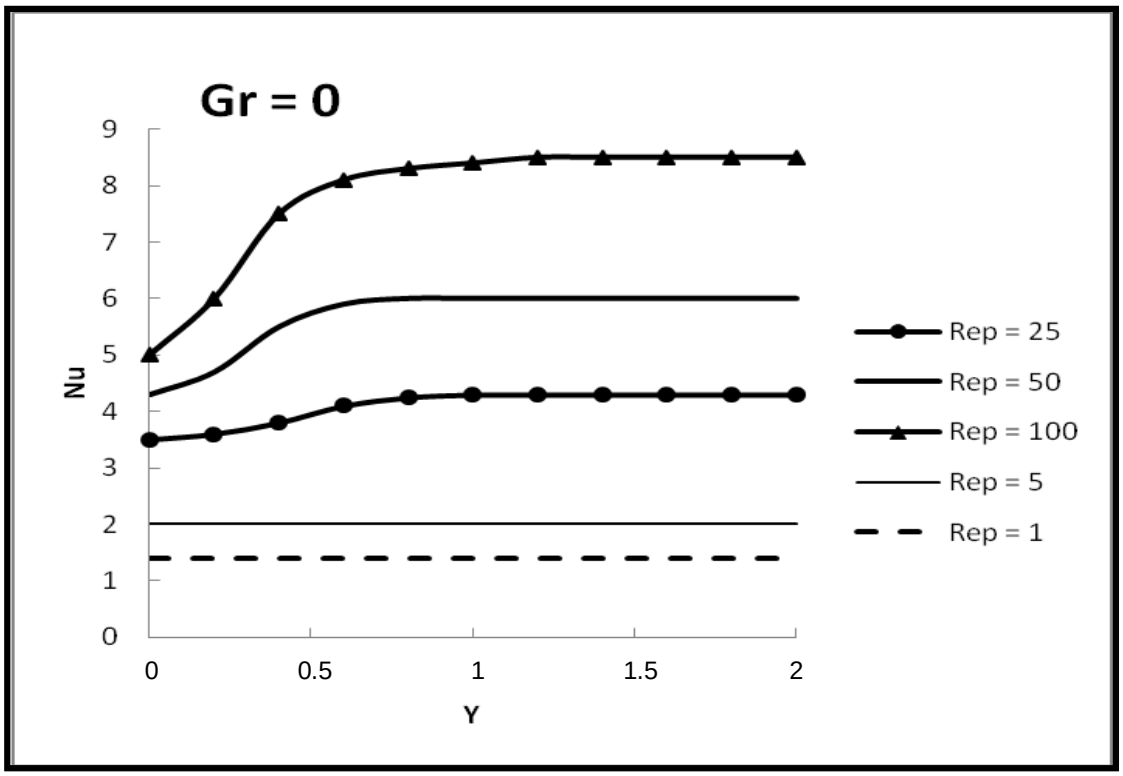

Figure 3. Nusselt number distributions, Gr = 0.

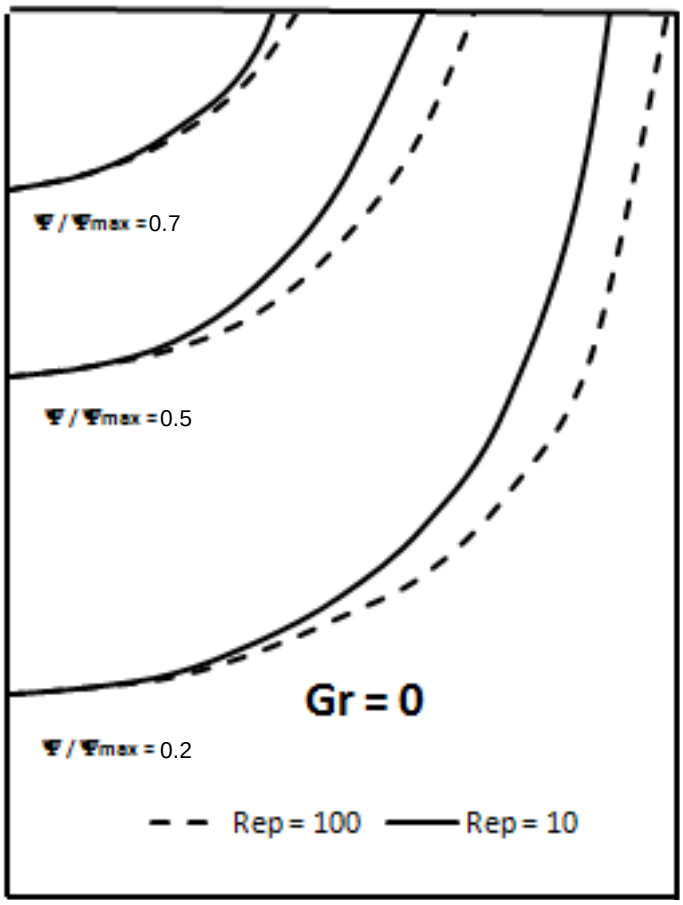

Figure 4. Comparison of streamlines (Ψ/Ψ_{max}) for Gr = 0.

the heated wall when Re increases. In view of the definitions of Nu in Equations (13) and (14), Figure 3 also indicates that h and θ attain uniform values. This thermal behaviour is analogous to that of the two-dimensional stagnation flow (Kays, 1966), mainly when Re_p is small in Figure 3. The increase of fluid flow along the height of the heated wall, due to injection at the permeable wall, causes a smaller thermal penetration into the fluid in the upper portion of the cavity, as indicated in Figure 5. It is evident in Figure 5 the larger thermal resistance near the bottom of the heated wall.

The effects of natural convection on the Nusselt number distributions will now be considered. The results obtained for a relatively low Re_p are show in Figure 6. The curves of Nusselt number distributions are parametrized with the modified Grashof number. For the smallest values of Gr (10 and 100), the distributions are very similar to those shown in Figure 3. In this range of Gr the mechanism of forced convection is still dominant. The isotherms in the fluid are similar to those of Figure 5 and the heated wall thermal resistance is higher near the bottom of the cavity. As the Grashof number increases, there is an enhancement of heat transfer so that, as indicated in Figure 6, the entire heated plate becomes colder. The effects of the buoyancy forces, acting mainly close to the heated wall, share the dominant role on heat transfer with the forced convection effects. The Nusselt number profiles for Gr larger than 10^3 in Figure 6 indicate that the wall temperature initially decreases slightly from the bottom of the cavity and attains downstream a minimum value. The behaviour is distracted by forced convection effects. The minimum wall temperature occurs however, on the lower portion of the cavity instead of on the upper portion, as was the case in Figure 3. Downstream of this minimum, the wall temperature now increases monotonically to the upper end of the cavity. This behaviour is imposed by natural convection effects. The values of the Gr in Figure 6 are limited in the upper range ($Gr < 10^4$) due to the condition of no backflow of fluid at the outflow boundary. In this respect, the effects of natural convection are somewhat restrained for the relatively low value of Re_p in this figure.

The streamlines and isotherms for Re_p = 5 and Gr = 3,000 are showed in Figure 7. Due to the buoyancy induced flow, the streamlines, compared to the case for Gr = 0 in Figure 4, penetrate deeper into the cavity before

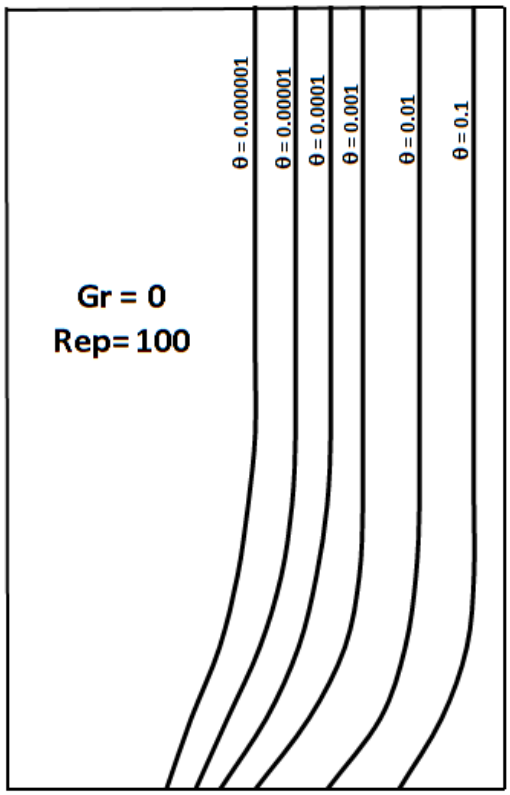

Figure 5. Isotherms for Gr = 0 and Re_p = 100.

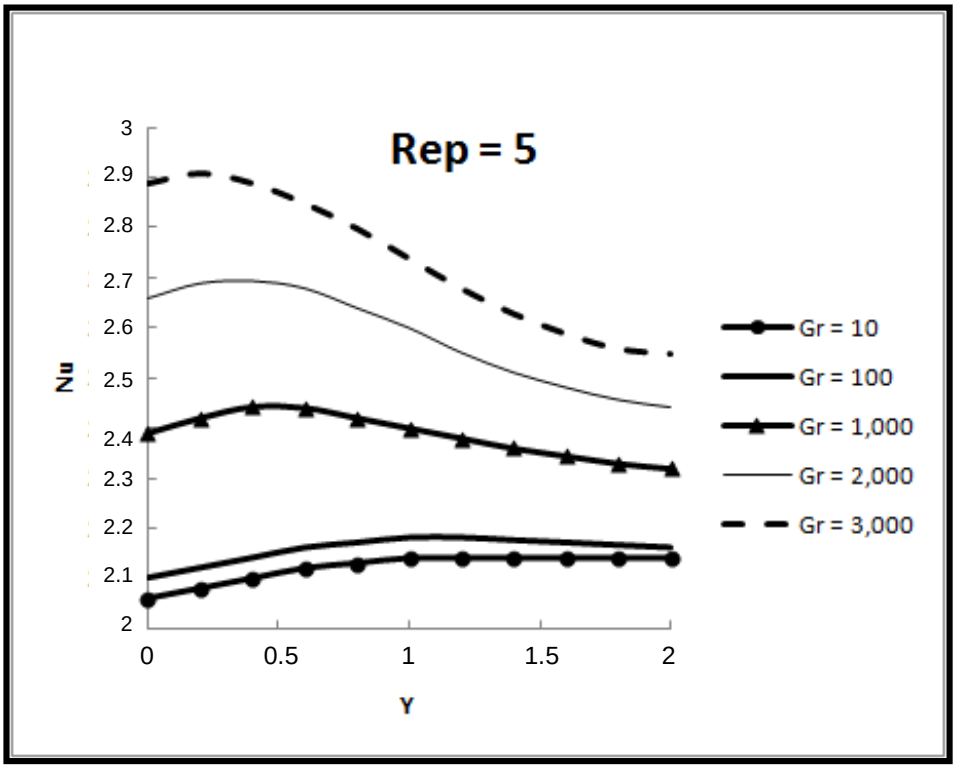

Figure 6. Nusselt number distributions, Re_p = 5.

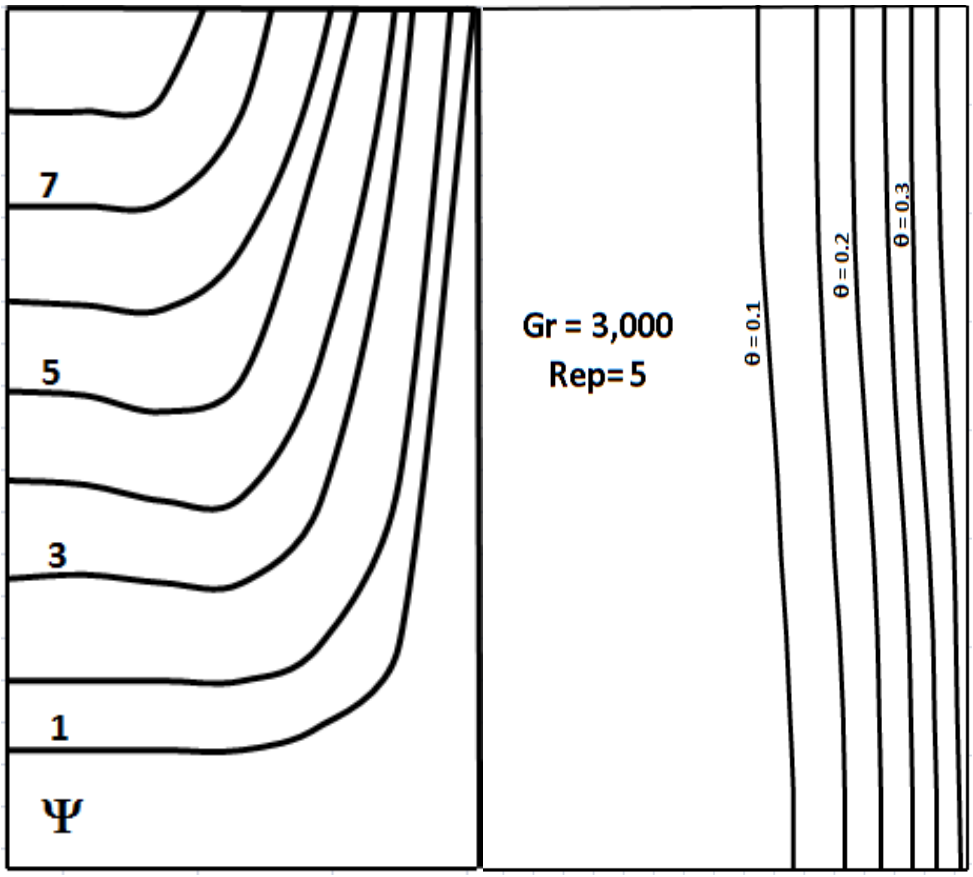

Figure 7. Streamlines and Isotherms for $Re_p = 5$ and Gr = 3,000.

bending upward. Thus, a large portion of the fluid flow leaves the cavity near the heated wall. The isotherms presented in the same figure give a clear indication of the development of a natural convection boundary layer along the heated wall. It is also noticed an increase of the heated wall thermal resistance very convection effects still predominate.

The Nusselt number distributions for a relatively high Re_p are now shown in Figure 8. Again, for small values of Gr, there is almost no distinction from the case in the absence of natural convection effects. With this Re_p, the parameter Gr can be increased to a much higher value than before without any backflow of fluid at the outflow boundary. For the largest values of Gr in Figure 8, the heated wall temperature is a minimum right at the bottom and increases monotonically along its length. In this case, the natural convection effects control the heat transfer. The streamlines and isotherms shown in Figure 9 correspond to Re_p equal to 30 and Gr = 10^6. The streamlines indicate that now half of the flow leaves the cavity within only 10% of its width, near the heated wall. The streamlines at the bottom go almost straight to the heated wall. The induced buoyant flow causes a bending of these lines slightly downward before turning upward. The isotherms indicate a natural convection boundary layer development form the bottom of the heated wall. There is no increase in the thermal resistance of wall near the bottom of the cavity, as shown by the isotherms closest to the heated wall.

Average Nusselt numbers

The average Nusselt numbers are shown in Figure 10 as function of Re_p and parametrized with the modified Grashof number. The relative enhancement of heat transfer due the effects of natural convection decreases with Re_p. For the largest value of Gr in Figure 10, equals to 10^7, the effects of natural convection are so dominant that the value of Nu is almost independent of Re_p for the range investigated.

Another view is presented in Figure 11, where Nu is shown as a function of Gr and parametrized with respect to Re_p. It is clear that the enhancement of heat transfer by natural convection occurs when Gr attains a minimum value. This Gr seems to increase slightly with Re_p. As noticed before, Nu attains a limit value practically independent of Re_p.

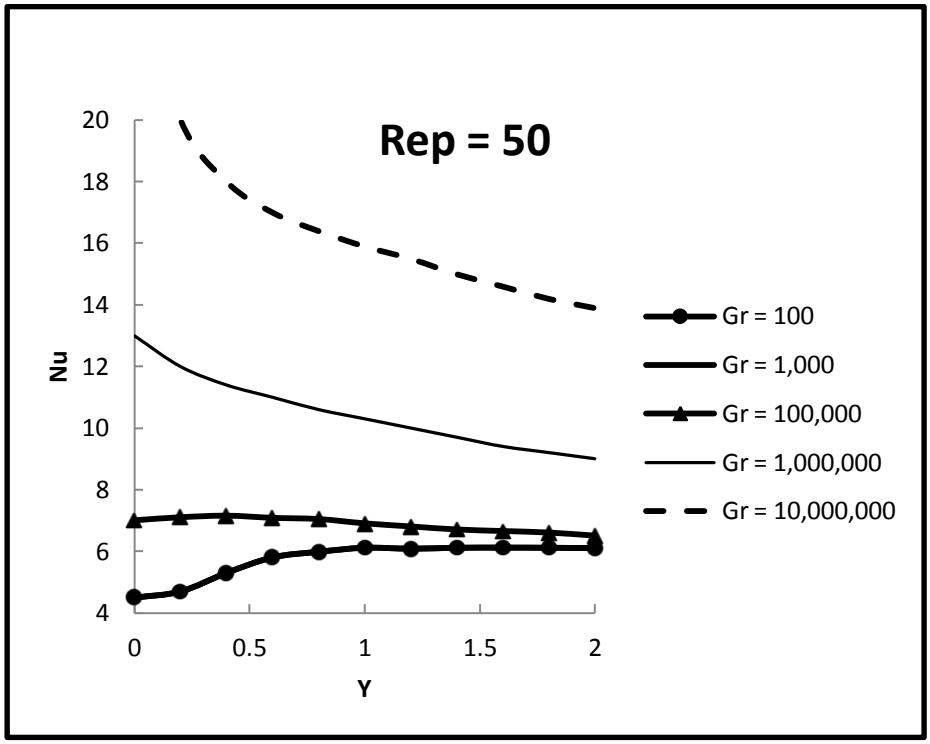

Figure 8. Nusselt number distributions, $Re_p = 50$.

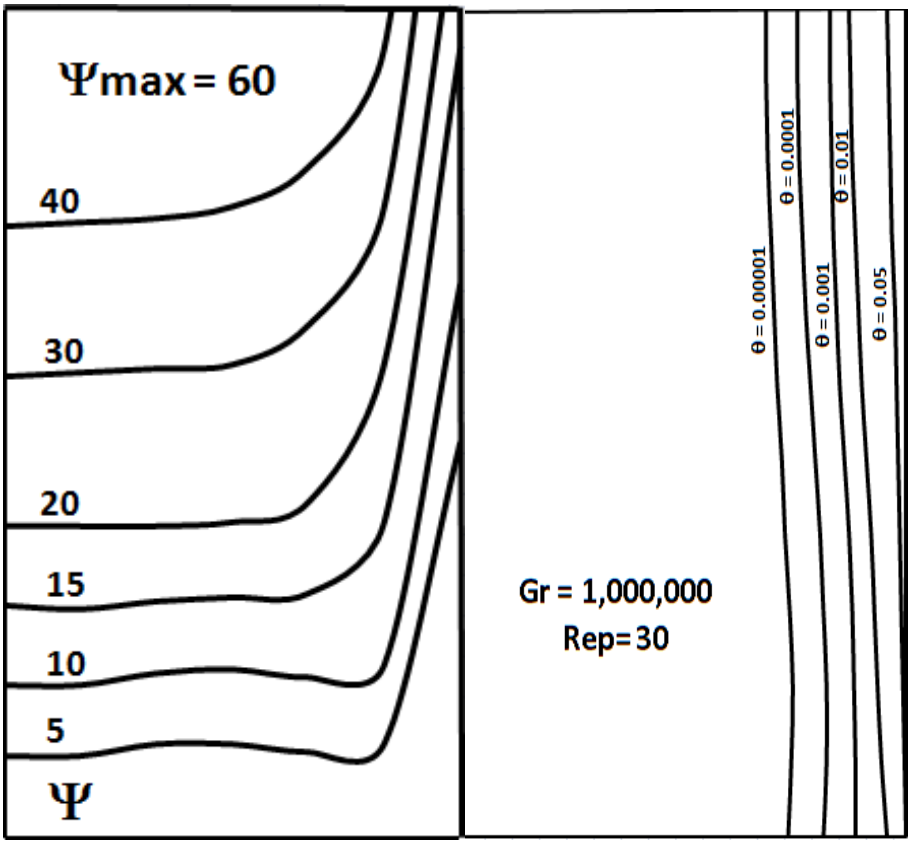

Figure 9. Streamlines and Isotherms for $Re_p = 30$ and $Gr = 10^{6.}$

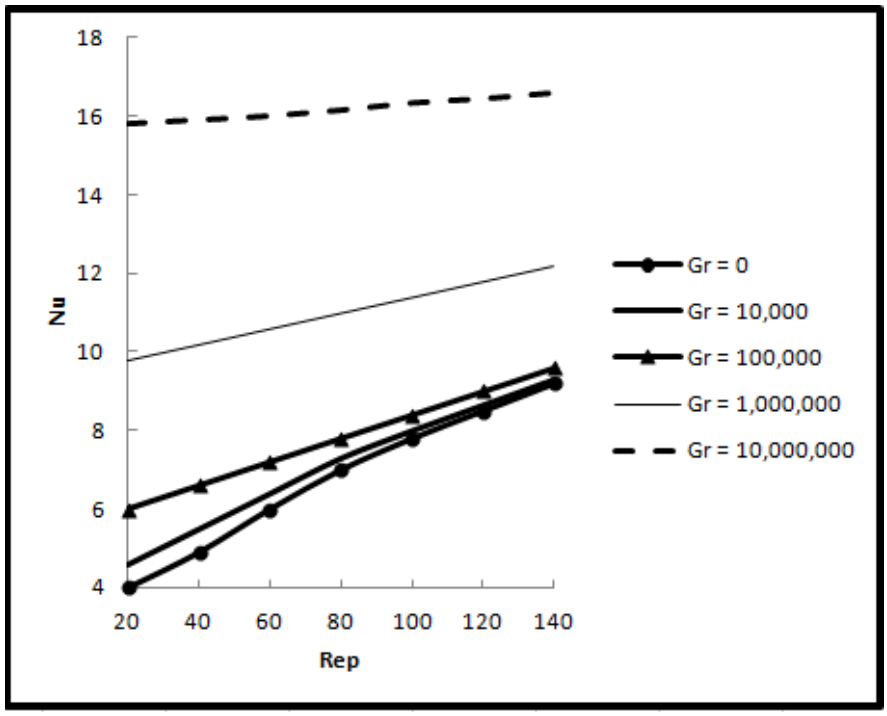

Figure 10. Average Nusselt numbers as a function of Re_p.

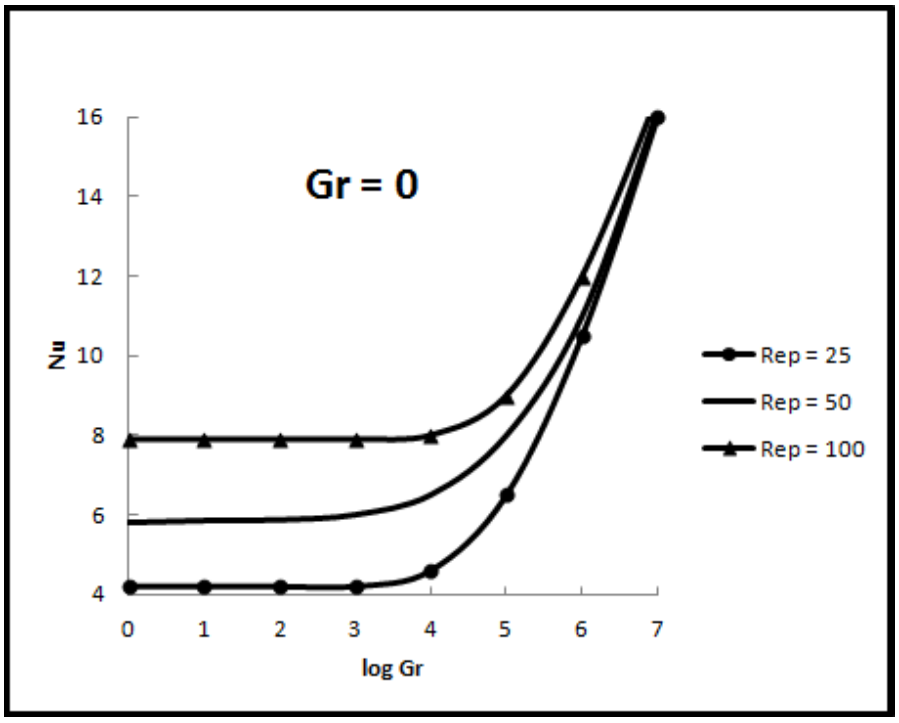

Figure 11. Average Nusselt numbers as a function of Gr.

Aspect ratio

The results presented so far were obtained for an aspect ratio (H/D) of the open cavity equal to 2. In Figure 12, the Nusselt number distributions for the aspect ratios of 2, 4 and 8, obtained for a pair of values of Re_p and Gr, are

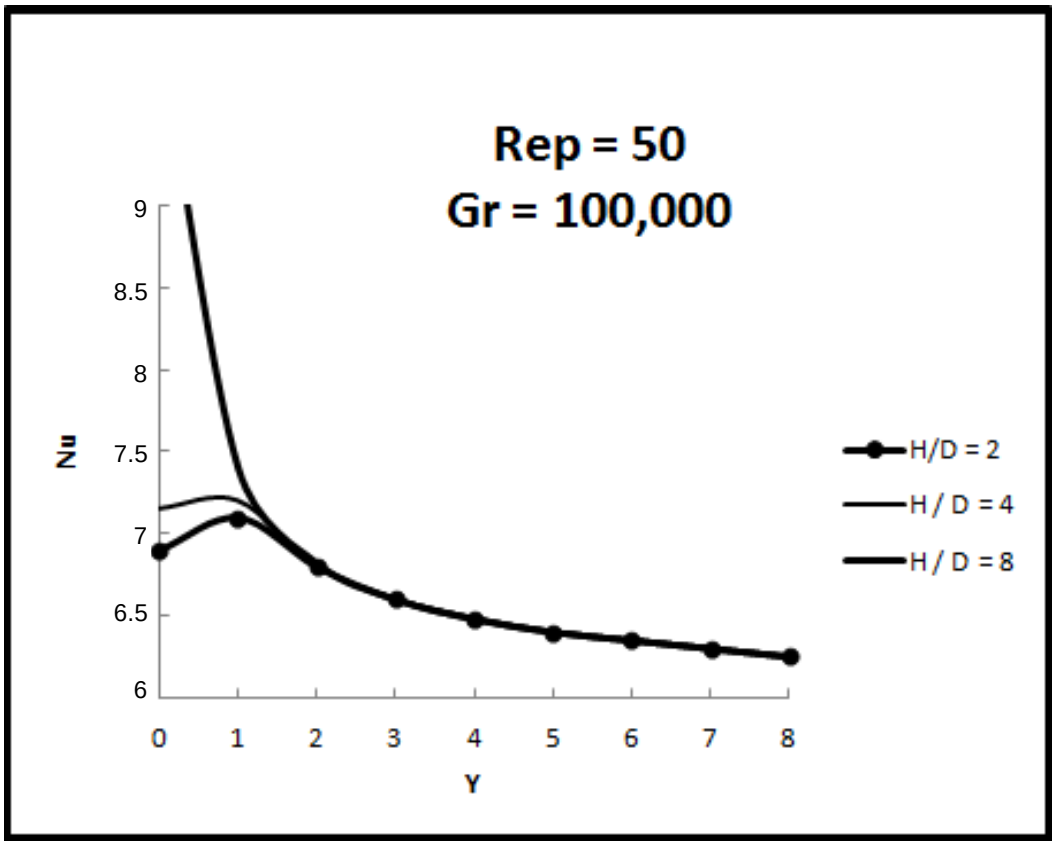

Figure 12. Influence of the aspect ratio.

compared. The distribution for (H/D) equal to 2 is the same as that included in Figure 7, but in a much enlarged vertical scale. As the aspect ratio increases, the minimum temperature of the heated wall moves closer to the bottom of the cavity. As discussed before, this temperature characterizes the start up of a natural convection boundary layer along the heated wall. Thus, these profiles indicate a stronger effect of natural convection as the aspect ratio of the cavity increases. It is also noticed that the Nusselt number distributions in the region controlled by natural convection match each other. In this region the heated wall temperature distributions seem to be independent of the aspect ratio of the cavity.

Conclusions

The study of laminar free and forced convection cooling of a semi permeable open cavity was investigated numerically. The equations describing the problem were expressed in Cartesian coordinates according to stream function formulation and numerically solved by the method of control volume. The program implemented allowed to achieve satisfactory results and enabled a better understanding of the influence of Reynolds and Grashof numbers on flows driven by heat. The results obtained show that the forced convection inside the semi-porous open cavity studied may be greatly enhanced by natural convection effects. When Gr is small enough, just forced convection controls the heat transfer. In this case, the upper portion of the heated plate becomes the most convenient region for cooling purposes. When Gr increases, natural convection effects may become dominant and then the lower portion of the heated plate constitutes the coldest region. When the aspect ratio of the open cavity increases there seems to be an increase of the role played by natural convection effects. The investigation carried out was however, limited because the problem presents four parameters (H/D, Pr, Re_p and Gr) and some choices had to be made about the range to be analysed.

Conflict of Interest

The authors have not declared any conflict of interest.

Nomenclature: C_p, Specific heat at constant pressure [J/kg.^{o}C]; **D,** Width of the open cavity [m]; **g,** Acceleration

of gravity [m/s^2]; **Gr,** Modified Grashof number [-]; $\overline{h}$ **,**Convective heat transfer coefficient [W/m^2.°C]; **H,** Height of the open cavity [m]; **Nu,** Local Nusselt number [-]; $\overline{Nu}$ **,**Average Nusselt number [-]; **p,** Pressure [Pa]; **p*,** Modified pressure [Pa]; **P,** Dimensionless pressure [Pa]; **Pr,** Prandtl number of the fluid [-]; **q,** Surface heat flux [W/m]; **Re$_p$,** Porous wall Reynolds number [-]; **T,** Temperature [°C]; **T$_p$,** Temperature of the porous wall [°C]; **T$_w$,** Heated wall temperature [°C]; $\overline{T}_w$ **,** Average temperature of the heated wall [°C]; **u$_p$,** Injection velocity of fluid at the porous wall [m/s]; **U, V,** Dimensionless velocities [m/s]; **x, y,** Cartesian coordinates [m]; **X, Y,** Dimensionless Cartesian coordinates [m]; **β,** Coefficient of thermal expansion [1/°C]; **ψ,** Stream function [-]; **ν,** Kinematic viscosity [m^2/s]; **θ,** Dimensionless temperature [°C]; θ_w **,** Dimensionless heated wall temperature [°C]; $\overline{\theta}_w$ **,** Dimensionless average heated wall temperature [°C]; **ρ,** Density [kg/m]; **Σ,** Number of grid points in the domain [-]; **μ,** Viscosity [Pa.s]; **κ,** Thermal conductivity [W/m. °C].

REFERENCES

Altemani CAC, Chaves CA (1988). Convective cooling of a semiporous open cavity. In: XXVI National Heat Transfer Conference, Heat Transfer in Electronics – HTD: ASME, Philadelphia, 111:149-154.

Bairi A, Garcia de Maria JM, Bairi I, Laraqi N, Zarco-Pernia E, Alilat N (2012). 2D transient natural convection in diode cavities containing an electronic equipment with discrete active bands under constant heat flux. Int. J. Heat Mass Transfer 55(19-20):4970-4980.

Bairi A, Laraqi N, Garcia de Maria JM (2007). Numerical and experimental study of natural convection in tilted parallelepipedic cavities for large Rayleigh numbers. Exp. Therm. Fluid Sci. 31(4):309-324.

Bejan A (1984). Convection Heat Transfer. New York, NY: Wiley Interscience,

Boukhanouf R, Haddad A (2010). A CFD analysis of an electronics cooling enclosure for application in telecommunication systems. Appl. Therm. Eng. 30(16):2426-2434.

Bruchberg H, Catton I, Edwards DK (1976). Natural convection in enclosed spaces: a review of applications to solar energy collection. ASME J. Heat Transfer. 98:182-188.

Chan YL, Tien CL (1985). A numerical study of two-dimensional laminar natural convection in shallow open cavities. Int. J. Heat Mass Transfer. 28:603-612.

Chaves CA, Camargo JR, Cardoso S, Macedo AG (2005). Transient natural convection heat transfer by double diffusion from a heated cylinder buried in a saturated porous medium. Int. J. Therm. Sci. 44:720-725.

Chaves CA, Camargo JR, Correa VA (2008). Combined forced and free convection heat transfer in a semiporous open cavity. Sci. Res. Essay. 3(8):333-337.

Farid SK, Billah MM, Rahman MM, Sharif UMd (2013). Numerical study of fluid flow on magneto-hydrodynamic mixed convection in a lid driven cavity having a heated circular hollow cylinder. Procedia Eng. 56:474-479.

Fontana E, Silva A, Mariani VC (2011). Natural convection in a partially open square cavity with internal heat source: An analysis of the opening mass flow. Int. J. Heat Mass Transfer 54(7–8):1369-1386.

Gandhi MS, Ganguli AA, Joshi JB, Vijayan PK (2012). CFD simulation for steam distribution in header and tube assemblies. Chem. Eng. Res. Design 90(4):487-506.

Hess CF, Henze RH (1984). Experimental investigation of natural convection losses from open cavities. ASME J. Heat Transfer 106:33-338.

Juarez JO, Hinojosa JF, Xaman JP, Tello MP (2011). Numerical study of natural convection in an open cavity considering temperature-dependent fluid properties. Int. J. Therm. Sci. 50(11):2184-2197.

Kakaç S, Shah RK, Aung W (1987). Handbook of Single Phase Convective Heat Transfer. New York, NY: John Wiley & Sons,

Kays WM (1966). Convective Heat and Mass Transfer. New York, NY: McGraw-Hill.

Kundu PK, Cohen IM (2008).Fluid Mechanics. 4 ed. New York, NY: Academic Press.

Nickell T (1997). Cooling analysis eliminates fan, reducing weight by 60 % and power draw by 75%. Simulation 68(5):301-303.

Ostrach S (1972). Natural Convection in Enclosures. Adv. Heat Transfer 8:161-227.

Patankar SV (1980). Numerical Heat Transfer and Fluid Flow. New York, NY: McGraw-Hill – Hemisphere.

Penot F (1982). Numerical calculation of two-dimensional natural convection in isothermal open cavities. Numer. Heat Transfer 5:421-437.

Prakash M, Kedare SB, Nayak JK (2012). Numerical study of natural convection loss from open cavities. Int. J. Therm. Sci. 51(1):23-30.

Rahman MM, Saidur R, Rahim NA (2011). Conjugated effect of joule heating and magneto-hydrodynamic on double-diffusive mixed convection in a horizontal channel with an open cavity. Int. J. Heat Mass Transfer 54(15-16):3201-3213.

Shaalan MR, Saleh MA, Mesalhy O, Elsayed ML (2012). Thermo/fluid performance of a shielded heat sink. Int. J. Therm. Sci. In Press, Corrected Proof, Available online 23 June. pp. 1-11.

Sharma PK (2005). Fluctuating thermal and mass diffusion on unsteady free convection flow past a vertical plate in slip-flow regime. Lat. Am. Appl. Res. 35(4):313-319.

Sparrow EM, Stryker PC, Altemani CAC (1985). Heat transfer and pressure drop in flow passages that open along their lateral edges. Int. J. Heat Mass Transfer 28(4):731-740.

Stiriba Y, Ferre JA, Grau FX (2013). Heat transfer and fluid flow characteristics of laminar flow past an open cavity with heating from below. Int. Commun. Heat Mass Transfer 43:8-15.

Stiriba Y, Grau FX, Ferre JA, Vernet A (2010). A numerical study of three-dimensional laminar mixed convection past an open cavity. Int. J. Heat Mass Transfer 53(21-22):4797-4808.

Wong K-C, Saeid NH (2009). Numerical study of mixed convection on jet impingement cooling in an open cavity filled with porous medium. Int. Commun. Heat Mass Transfer 36(2):155-160.